ACS APPLIED ELECTRONIC MATERIALS

pubs.acs.org/acsaelm Letter

An Organic Retinomorphic Sensor

Cinthya Trujillo Herrera and John G. Labram*

Cite This: https://doi.org/10.1021/acsaelm.1c00955 Read Online

ACCESS | Metrics & More | Article Recommendations | Supporting Information

ABSTRACT: Inspired by the way retinal cells respond to light, retinomorphic sensors are hoped to enable rapid identification of moving objects. Unlike conventional optical sensors, these sensors are designed to produce a signal in response to changes in illumination but not under constant illumination. This report represents the first demonstration of a retinomorphic sensor employing organic semiconductors as the absorber. The sensor exhibits stability under constant measurement conditions up to a period of 1 h and characteristic decay times that are tunable through a choice of external resistor, demonstrated down to 10 μs, roughly 10 000 times faster than previous devices.

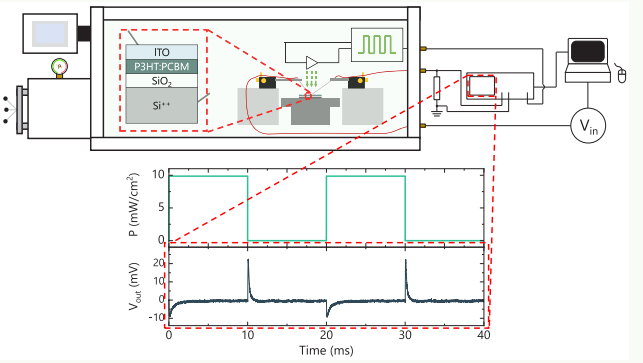

KEYWORDS: *retinomorphic, neuromorphic, event-driven, organic semiconductor, optical sensor*

Currently, the analysis of visual information occurs almost[1] exclusively in processors,[2] with data provided as a series of conventional images, such as a two-dimensional (2D) arrays of intensity (e.g., bitmaps). Because of restrictions due to frame rate and processing time, the speed at which moving objects can be identified using conventional cameras is fundamentally limited. Most cameras employ a 2D array of complementary metal oxide semiconductor (CMOS) or charged coupled device (CCD) sensors, both utilizing photodiodes to detect light. A photodiode will output a signal (current) that depends on the intensity of light that falls upon it.[3] Unlike photodiodes, animal retinas produce a stronger signal in response to time-varying visual stimuli than to static images.[4,5] This results in a large volume of nonpertinent information being filtered out by the eye, before it reaches the brain.

We recently demonstrated sensors inspired by this strategy.[6] Our so-called *retinomorphic sensors* employed a metal halide perovskite[7] absorber layer as one layer of a bilayer dielectric, in a photosensitive capacitor. When placed in series with a resistor and a voltage is applied across the resistor−capacitor circuit, the device was found to output a voltage in response to changes in illumination but produced zero voltage under constant illumination. The behavior was tested by applying a step change in optical power density, resulting in a spike in output voltage followed by a monoexponential decay.

While a valuable proof-of-concept demonstration, our initial sensors had two serious drawbacks. First, the semitransparent gold top contact had to be thin (15 nm) to enable optical access to the absorber layer. This thin film of gold on a polycrystalline surface resulted in a very high contact resistance, which in turn caused a large decay constant (on the order of 100 ms) that could not be controlled through a choice of external resistor. Second, the device exhibited significant instability under constant bias. Specifically, the magnitude of the output voltage spike changed as a function of time. Bias-stress instabilities are widely observed in metal halide perovskite solar cells[8] and often attributed to a voltage-induced redistribution of mobile ions.[9] We interpret our observations as being analogous to those observed in metal halide perovskite field effect transistors (FETs),[10] where ionic screening is believed to inhibit electronic charge accumulation.[11]

Here, we present an alternative device structure, employing an organic semiconductor blend as the absorber layer and a transparent conducting oxide (TCO) as the top electrode. TCOs combine high electrical conductivity with high optical transparency[12] and are widely employed in solar cells as transparent electrodes.[13] In our devices, they enable much thicker electrodes to be deposited than with gold, potentially reducing contact resistance. Organic semiconductors are more mature[14] and generally exhibit better stability[15] than metal halide perovskites. Importantly, because our retinomorphic sensors produce a signal as a result of changes in capacitance, not current flow, charges only have to be present, and not necessarily mobile, to contribute to the output voltage.[16] This suggests that while the mobility of charge carriers in organic

Received: October 4, 2021
Accepted: December 21, 2021

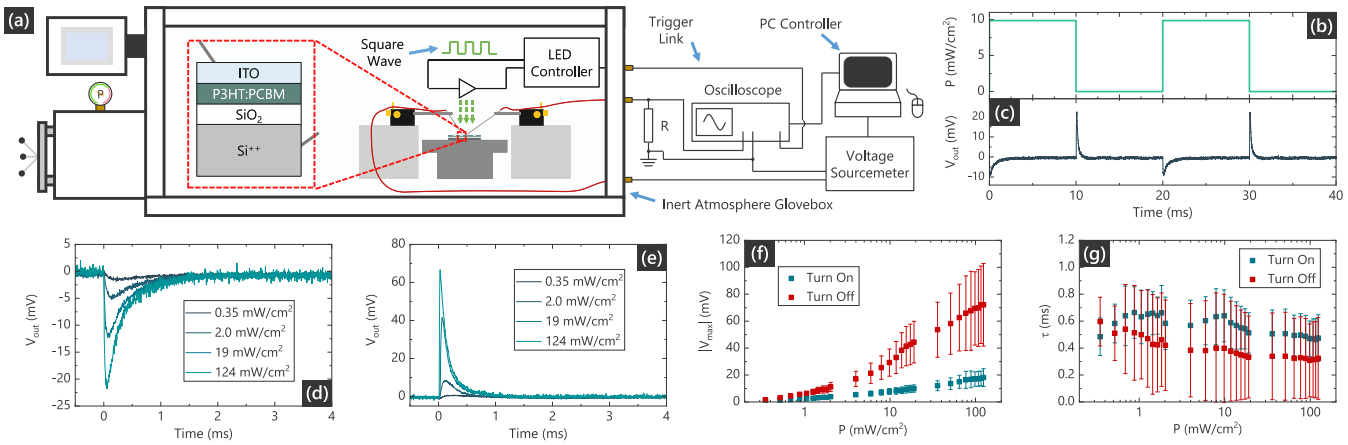

Figure 1. (a) Schematic illustration of device design and experimental setup used to measure organic retinomorphic sensors. Abbreviations: ITO = indium tin oxide, P3HT = poly(3-hexylthiophene-2,5-diyl), PCBM = phenyl-C_{61}-butyric acid methyl, SiO_2 = silicon dioxide, Si^{++} = highly doped silicon, LED = light emitting diode, PC = personal computer. (b) Example form of optical power density (P) incident on a photosensitive capacitor as a function of time. (c) Example response of an organic retinomorphic sensor, voltage across the resistor (V_{out}) as a function of time, in response to the incident square wave P. (d) Example response of an organic retinomorphic sensor to a step change increase in incident optical power density from 0 to P, at time = 0, for various values of P. (e) Example response of an organic retinomorphic sensor to a step change decrease in incident optical power density from P to 0, at time = 0, for various values of P. (f) Mean maximum magnitude of output voltage, $|V_{max}|$, of three different organic retinomorphic sensors as a function of P. Error bars denote standard deviation between devices. (g) Mean decay constant of $|V_{out}|$ of three organic retinomorphic sensors, τ, as a function of P, extracted assuming a monoexponential decay. Error bars denote standard deviation between devices. V_{in} = 5 V and R = 100 kΩ in all cases.

semiconductors is often at least an order of magnitude lower than it is in metal halide perovskites,[17,18] it is also expected to be a much less influential parameter in retinomorphic sensors than in organic FETs (OFETs) or organic photovoltaics (OPVs), where charges must travel through the material to contribute to current.

A depiction of our device structure and measurement setup is depicted in Figure 1(a). The capacitor consists of a highly doped silicon (Si) bottom electrode, an indium tin oxide (ITO) top electrode, and a bilayer dielectric. The bottom layer of the dielectric is silicon dioxide (SiO_2), which is highly resistive, stable, and irresponsive to optical illumination.[19] The top layer of the dielectric is a 50:50 (weight %) blend of the p-type polymer poly(3-hexylthiophene-2,5-diyl) (P3HT) and the n-type small molecule phenyl-C_{61}-butyric acid methyl (PCBM). Organic semiconductor blends such as P3HT:PCBM are strong absorbers of visible light[20] and are studied extensively for use in solar energy conversion[21,22] and optical detection.[3,23] Photographs of the device are shown in Figure S1.

To test these devices, they were placed in series with a conventional resistor of resistance R, and a constant input voltage (V_{in}) was applied across the capacitor−resistor circuit. Light was applied to the capacitor as a square wave of frequency f, with an incident optical power density between 0 and P. The voltage across the resistor (V_{out}) was measured as a function of time with an oscilloscope.

An example of the waveform applied to the capacitor is shown in Figure 1(b), and the resulting sensor output is shown in Figure 1(c). Here, R = 100 kΩ, f = 50 Hz, and V_{in} = 5 V. We see that the sensor produces the desired behavior: a spike in voltage when the light is turned on or off, but otherwise, the voltage is close to 0 V. Unexpectedly, we observe that V_{out} is negative when the light turns on and positive when the light turns off. Additionally, the magnitude of the spike is asymmetric between turn-on and turn-off signals. These unexpected results are discussed toward the end of this report.

As observed with our previous devices,[6,16] the magnitude of the voltage spike increased with increasing P. Figure 1(d) shows four examples of V_{out} as a function of time in response to a step change in light intensity from 0 to four different values of P. Figure 1(e) shows equivalent data in response to a step change reduction in light intensity from four different values of P to 0. Figure 1(f) shows the magnitude of the maximum value of V_{out}, denoted $|V_{max}|$, as a function of P, for three identically prepared devices. The individual $|V_{max}|$ vs P response of the three devices is shown in Figure S2. While the device-to-device variation is significant, the behavior is similar in all devices: a negative V_{out} as the light is turned on, a positive V_{out} as the light is turned off, and a larger $|V_{max}|$ when the device is turned off compared to when it is turned on.

We expect a number of device parameters to affect the magnitude of $|V_{max}|$ in response to a given value of P. Most notably, a thicker semiconductor is expected to absorb more light per unit area and also provide a lower dark capacitance, which we expect to yield a larger response.[16] Increasing the thickness is also anticipated to change the micromorphology of the semiconductor layer, a well-studied and complex topic in the field of organic semiconductor blends.[24] Because these devices rely on a capacitive effect rather than direct contribution to current, charges do not have to percolate to the electrode to contribute to the detected signal; they only have to be present. For this reason, we do not expect charge carrier mobility or microstructure to be as critical a factor as it is in solar cells or thin film transistors for example.

Further study is required, but we hypothesize that a thick film of a finely intermixed bulk heterojunction, formed of coevaporated donor and acceptor semiconductors,[25] could yield a strong response in these sensors. The number of donor and acceptor organic semiconductor molecules one can choose from is decidedly large.[26,27] We here chose to focus on the most well-studied[28] system: P3HT:PCBM. It is likely that future improvements in organic retinomorphic sensors will

https://doi.org/10.1021/acsaelm.1c00955
ACS Appl. Electron. Mater. XXXX, XXX, XXX−XXX

come from improving the electronic interface between these two components.

The decays were found to fit a monoexponential decay function (see Figure S4 for examples), from which a characteristic decay time (τ) could be extracted. The mean value of τ between the three devices is plotted as a function of P in Figure 1(g), with the individual response shown in Figure S3. As with $|V_{max}|$, variation in τ between devices was significant; however, all devices exhibited τ between 100 μs and 1 ms, a small decrease with increasing P and a slightly larger τ for turning on compared to turning off. An increase in bimolecular[29,30] and Auger[31] recombination at higher P is a possible explanation of the dependence of τ on P.

It is noteworthy that these new devices respond roughly 1000 times faster than our original device,[6] suggesting that the ITO top electrode has indeed reduced the contact resistance of the structure. This is because previously the R_C was much larger than the value of the external resistor, R, meaning that R_C always dominated the RC time constant, regardless of what value of R we chose in our circuit. Here $R_C \ll R$, suggesting that R now dominates, lowering τ. The values of τ shown in Figure 1(g) were all evaluated using the same external resistor, R = 100 kΩ. One attractive feature of retinomorphic sensors is that they should have a τ that is tunable through a choice of R. Figure 2(a) shows normalized $|V_{out}|$ as a function of time in response to turning the light on from 0 to P = 124 mW/cm^2, for four different values of R. Figure 2(b) shows the equivalent data when the light is turned off from P = 124 mW/cm^2 to 0. As expected, τ decreases as R decreases. Figure 2(c) shows τ as a function of resistance in response to both turning the light on and turning the light off. The rise time of $|V_{out}|$ was also approximated as a function of R in Figure S5. The rise time increased with R and was higher for when the light was turned on compared to when it was turned off.

In addition to τ, $|V_{max}|$ was also observed to decrease as R was decreased, as shown in Figure 2(d). This is expected for a device with a finite contact resistance, as the external resistor R and the contact resistance R_C will act as a potential divider, with only the voltage dropped across R being measurable as V_{out}. The dependence of $|V_{max}|$ on R was modeled using the equation for a potential divider and assuming a constant R_C for turn-on and a constant R_C for turn-off. These fits are shown as the lines in Figure 2(d). The fits yield values of 50 kΩ for turn-on and 31 kΩ for turn-off. The discrepancy between the two values and the suboptimal fit are likely due the fact that this simple model neglects the non-Ohmic nature of the injection barrier.[32] It nonetheless enables us to approximate R_C as being roughly 3 orders of magnitude lower than our previous device.[6]

The fastest τ measured here was 8 μs in response to the light turning on and 3 μs in response to the light turning off, comparable to the equivalent rise times. This suggests that such sensors could potentially resolve objects that spend <10 μs in the visual field, enabling tracking of extremely high velocity objects. It is anticipated that this number could be improved further by reducing the device area, increasing the SiO_2 and/or semiconductor thickness, or by optimizing the interfaces for a low R_C. A lower R_C could be achieved by depositing the ITO at an elevated temperature and hence reducing resistance[12] or by changing the electrode or semiconductor material in order to reduce the interfacial barrier height.[32]

One of the primary motivations for considering organic semiconductors rather than metal halide perovskites is that

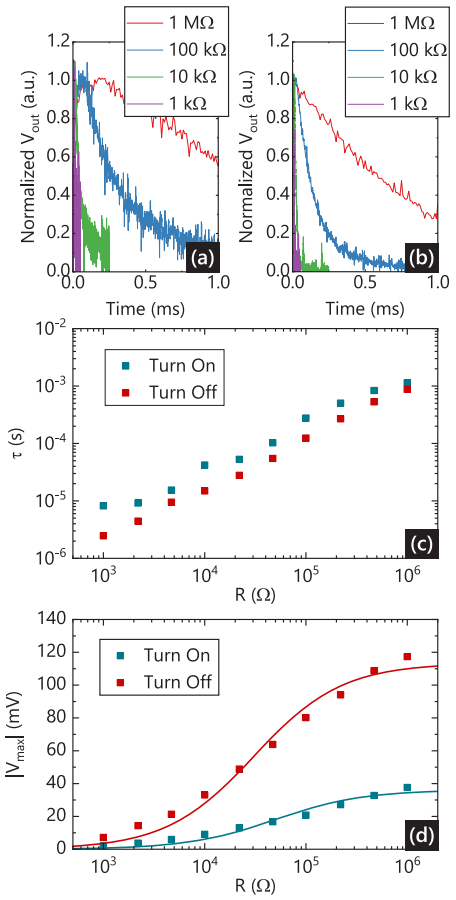

Figure 2. Output voltage, V_{out}, of an organic retinomorphic sensor measured as a time, normalized between 0 and 1, in response to a step change in optical power density (a) from 0 to P = 124 mW/cm^2 and (b) from P = 124 mW/cm^2 to 0, for various values of an external resistor, R. (c) Decay constant of an organic retinomorphic sensor, τ, as a function of R, extracted assuming a monoexponential decay, in response to light applied as step function from 0 to P = 124 mW/cm^2 ("Turn On") and from P = 124 mW/cm^2 to 0 ("Turn Off"). (d) Magnitude of peak output voltage, $|V_{max}|$, of an organic retinomorphic sensor as a function of R, in response to light applied as step function from 0 to P = 124 mW/cm^2 ("Turn On") and from P = 124 mW/cm^2 to 0 ("Turn Off"). The lines are fits to a simple potential divider model where the device is assumed to have a constant contact resistance. V_{in} = 5 V in all cases.

they are hoped to exhibit better stability under constant bias. This was tested by applying an input voltage V_{in} and a square wave of light and then measuring the magnitude of the peak output voltage as a function of time under continuous square-wave illumination and bias. This is shown in Figure 3(a). No significant variations in $|V_{max}|$, or the form of the V_{out} response (see Figure S6), were observed over a period of 1 h. The stability over 12 h is shown in Figure S7, illustrating that eventually the device will reduce peak height, which we attribute to heating and degradation of the semiconductor compounds. Longer term studies under various lighting conditions will be valuable in the future, but the primary purpose of the work is to demonstrate significant stability improvements over the metal halide perovskite-based sensor,[6] which was unstable after a matter of seconds. We also observe that the magnitude of peak height increases over the first 30 min in this experiment. This is attributed to a reduction in ambient laboratory light as the motion-sensitive lights in the

https://doi.org/10.1021/acsaelm.1c00955
ACS Appl. Electron. Mater. XXXX, XXX, XXX−XXX

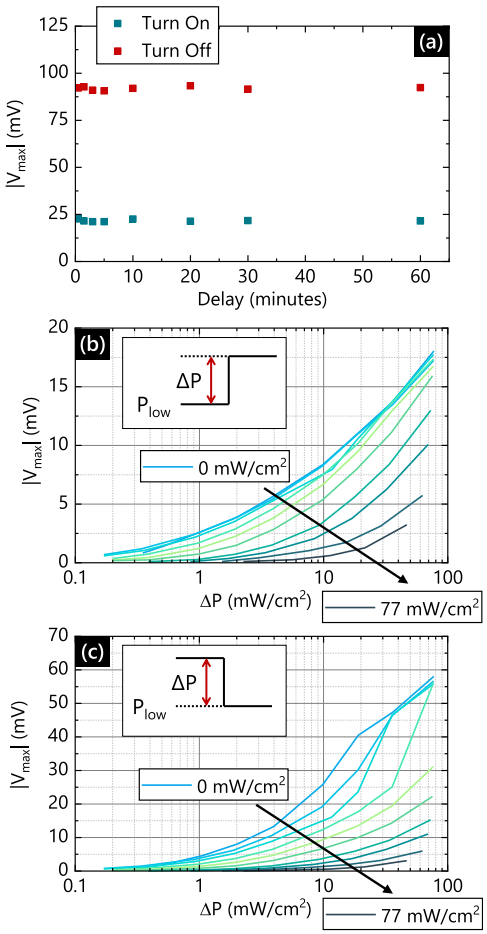

Figure 3. (a) Magnitude of peak output voltage, $|V_{max}|$, of an organic retinomorphic sensor as a function time after application of V_{in} = 5 V and a square wave of optical power density between 0 and P = 124 mW/cm^2. "Turn On" indicates the response to the light being applied, and "Turn Off" indicates the response to the light being withdrawn. (b) Magnitude of peak output voltage, $|V_{max}|$, of an organic retinomorphic sensor in response to an increase in light intensity from P_{low} to P_{low} + ΔP as a function of ΔP. (c) Magnitude of peak output voltage, $|V_{max}|$, of an organic retinomorphic sensor in response to a decrease in light intensity from P_{low} + ΔP to P_{low} as a function of ΔP. Values in legends for (b) and (c) denote P_{low}. V_{in} = 5 V and R = 100 kΩ in all cases.

laboratory turned off. A dedicated lightbox will hence be a useful strategy to carry out stability measurements in the future.

Up until now, these sensors have only been tested with very low background light intensities (ambient laboratory light), approximated as 0 mW/cm^2. For real world applications, it will be important to produce signals in response to changes between two nonzero power densities. Figure 3(b) shows the measured $|V_{max}|$ as a result of discontinuously increasing the incident optical power density from a low value (P_{low}) to a high value (P_{low} + ΔP), as a function of ΔP. Equivalent data is shown in Figure 3(c) for a step change from P_{low} + ΔP to P_{low}. This was carried out for a range of P_{low}, between 0 and 77 mW/cm^2. The strength of the output signal falls as P_{low} increases. This behavior is not unexpected, since the charge density in most semiconductors is known to obey a power-law relationship with optical power density,[33,34] implying that capacitance $C \propto P^{\gamma}$. Here, γ is a dimensionless exponent, which is close to 0.5 for systems dominated by bimolecular recombination.[35]

Finally, the response of these sensors was measured as a function of input voltage, V_{in}. Figure 4(a) shows $|V_{max}|$ measured as a function of V_{in}, in response to a step change in intensity between 0 and P = 124 mW/cm^2. Surprisingly, the magnitude of the peak and the general form of response (see Figure S8) were largely insensitive to the applied voltage. Even when V_{in} = 0, i.e., when the top electrode was grounded, the same response was observed. This is in contrast to our metal halide perovskite sensors, where input voltage was observed to significantly affect the output voltage.[6]

Control measurements were carried out with the P3HT:PCBM layer omitted from the structure but with otherwise equivalent conditions. The results are shown in Figure S9(a). A small positive V_{max} is observed when the light is turned on, and a small negative V_{max} is observed when the light is turned off (the opposite signs to when the P3HT:PCBM is present). The magnitude of these voltages however is approximately $|V_{max}| \approx 500\ \mu$V, roughly 100 times smaller than when the P3HT:PCBM is present. Peaks of a similar magnitude, and the same sign, are also visible when applying a very low light intensity (Figure S9(b)) or a very small change in light intensity (Figure S9(c)) to devices with the P3HT:PCBM present. For this reason, it is hypothesized that this phenomenon is likely to be an induction artifact due to the trigger signal (the cables ran in close proximity).

The observation that a nonzero V_{out} is produced, even when V_{in} = 0, means the original description applied to metal halide perovskite retinomorphic sensors was incomplete.[6,16] Our hypothesized mechanism for a grounded top electrode is shown in Figure 4(b–i). The mechanism relies upon the semiconductor having a dissimilar density of holes (p) and electrons (n) under constant illumination. This would be true if the monomolecular lifetimes of holes (τ_p) and electrons (τ_n) were unequal, for example as a result of asymmetries in trap density and/or depth. In the example depicted here, we have hypothesized that $\tau_p > \tau_n$, resulting in $p > n$ under constant illumination. Because the device is a capacitor, there only needs to be an asymmetry at the semiconductor–dielectric interface, not necessarily throughout the bulk. Bare SiO_2 is known to be a trap for electrons in OFETs,[36] and passivation is normally applied when n-type organic semiconductors are employed in OFETs with Si/SiO_2 substrates.[37] This means that it is possible that the density of electrons at the interface may be lower than holes, even if the bulk concentrations are comparable. We have here considered only a 1:1 P3HT:PCBM blend ratio, but we expect the blend ratio to strongly influence the relative number of holes and electrons under constant illumination and hence be a facile way to control the sign of V_{out} in response to various input stimuli.

The process of optical absorption and carrier generation in organic semiconductors is a complex topic,[38] but in general, free charge carriers are believed to be created ~100 fs to ~1 ps after photon absorption.[39,40] For most of the data obtained in this study, the period of the square wave ($1/f$) was ~10 ms. We can therefore approximate that charges are generated instantaneously when the light is applied. Recombination in bulk heterojunction solar cells is another detailed topic,[41] but we have observed lifetimes of free carriers in equivalently prepared P3HT:PCBM systems to be on the order of ~1 μs.[23] We can therefore also assume that $1/f$ is much longer than τ_p

https://doi.org/10.1021/acsaelm.1c00955
ACS Appl. Electron. Mater. XXXX, XXX, XXX–XXX

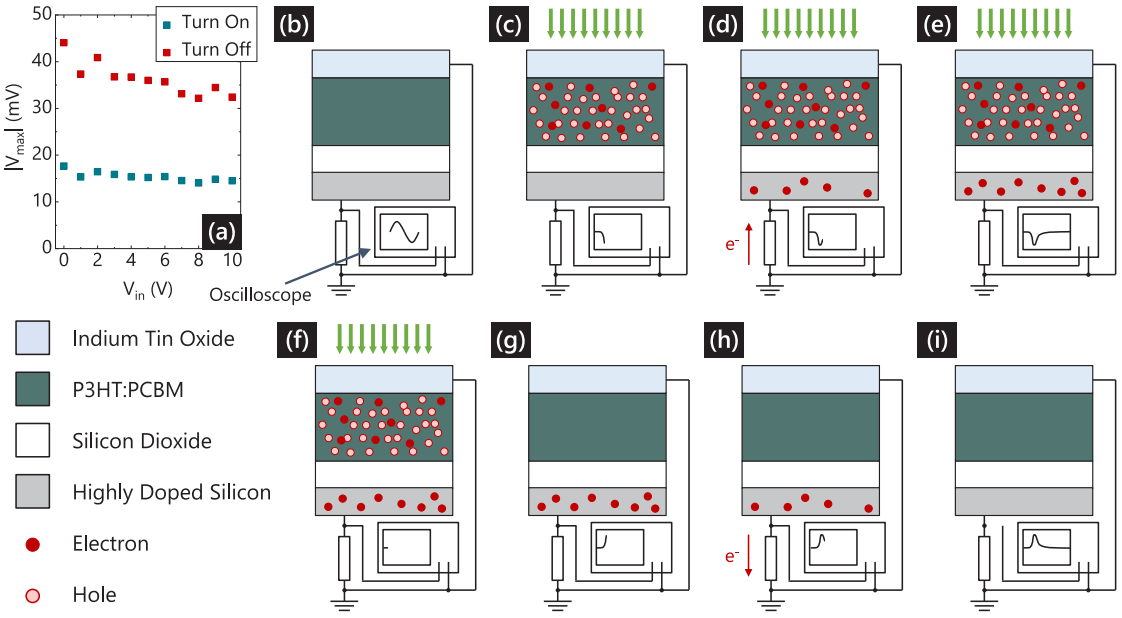

Figure 4. (a) Magnitude of peak output voltage, $|V_{max}|$, of an organic retinomorphic sensor as a function of input voltage, V_{in}, and square wave of optical power density in response to light applied as a step function from 0 to P = 124 mW/cm^2 ("Turn On") and from P = 124 mW/cm^2 to 0 ("Turn Off"), where R = 100 kΩ. Schematic illustration of the proposed operating mechanism for an organic retinomorphic sensor with a grounded top electrode in response to (b−e) application of light and (f−i) removal of light.

and τ_n for the cases where $R \gg 1$ kΩ, which is what we consider for this model.

The process is hypothesized to proceed as follows. When the light is incident, a roughly equal number of electrons and holes will be generated. However, since we assert that $\tau_p > \tau_n$, the system will soon equilibrate to steady-state conditions where $p > n$ (Figure 4(c)), leaving the semiconductor with a net positive charge. The net positive charge will create a driving force to pull electrons from ground to the bottom electrode or, equivalently, give the bottom electrode a lower potential relative to ground. This will be manifest as a negative V_{out}. Shortly after the potential on the bottom electrode is lowered, electrons will flow from ground through the resistor, onto the bottom electrode (Figure 4(d)), increasing the potential. This will continue to take place until the system returns to equilibrium and V_{out} returns to zero (Figure 4(e)). When the light is turned off, an analogous process is believed to occur. Before the light is removed, the system is in steady state with the bottom electrode and ground at the same potential (Figure 4(f)). We describe charges as recombining quickly relative to the RC time constant, which is a good approximation when R is large. With the net positive charge in the semiconductor now removed, the bottom electrode will have a positive potential relative to ground, and a positive V_{out} will be measured (Figure 4(g)). The electrons will then flow off the bottom electrode, through the resistor, to ground (Figure 4(h)), before equilibrating as the electrode becomes electrically neutral again (Figure 4(i)).

This description is consistent with our observation of a negative V_{out} when the light is applied and a positive V_{out} when the light is removed. We expect the opposite would be true if $\tau_p < \tau_n$. Our description is also consistent with the fast increase in $|V_{out}|$ when the light is applied or withdrawn, and a subsequent slower monoexponential decay in $|V_{out}|$, which depends on R. When R is low, say $\lesssim$1 kΩ, carrier recombination is anticipated to be comparable to the device decay time (τ). This would be expected to result in τ being comparable to the rise time in response to the light being removed (see Figure S5).

We acknowledge however that this model is likely to be oversimplified. It does not explain why the device is largely insensitive to V_{in}, as one would expect an applied bias to lead to a redistribution and injection/extraction of charge across the top electrode. We do observe a small decrease in peak height with increasing V_{in}, which we attribute to a bias-induced modification of the injection barrier between the ITO and P3HT:PCBM. The bias may be less influential if $p > n$ at the semiconductor/dielectric interface only, and elsewhere $p \approx n$, leading to a low charge flow between the ITO and P3HT:PCBM.

The reason behind the asymmetry of $|V_{out}|$ when the light is turned on and when the light is turned off remains unclear. It is possible that the time scales involved in reaching steady state are not the same as those for carrier recombination. We have carried out a simple simulation, described in Supporting Information Note S1 to investigate this briefly. This model is based on an analogous model we have previously used to verify steady state conditions in metal halide perovskites under constant illumination.[34] The results are shown in Figure S10, illustrating that the processes do occur over comparable time scales, but the form of the rise/decay is distinct. However, further study will be required to understand this feature more conclusively.

In conclusion, we have demonstrated a spiking retinomorphic sensor that employs an organic semiconductor as the absorber layer and a transparent conducting oxide as the top electrode. These devices were observed to be highly stable under constant bias conditions and produced a reproducible and consistent response to a step change in illumination. The devices exhibited a decay time that was controllable through the choice of external resistor R, with a minimum response time < 10 μs. Unexpectedly, these sensors were found to produce the desired response even without an applied input voltage. This result was rationalized by a simple model where

https://doi.org/10.1021/acsaelm.1c00955
ACS Appl. Electron. Mater. XXXX, XXX, XXX−XXX

the lifetimes of holes and electrons in the semiconductor were dissimilar. This is potentially highly desirable as it could enable the RC circuit to be fabricated as an integrated vertical two-terminal device, rather than a three-terminal device, as originally thought.[6] This could make sensor arrays less complex to fabricate and enable higher density.

■ ASSOCIATED CONTENT

Supporting Information

The Supporting Information is available free of charge at https://pubs.acs.org/doi/10.1021/acsaelm.1c00955.

> Methods, photographs of sensors, output voltage vs incident optical power density for individual sensors, decay constant vs incident optical power density for individual sensors, fit of monoexponential decay to voltage decay, approximation of rise time, output voltage as a function of time under constant measurement conditions, peak output voltage as a function of time under constant measurement conditions for 12 h, voltage as a function of time for various input voltages, control data, and simulation of charge generation and recombination in the semiconductor (PDF)

■ AUTHOR INFORMATION

Corresponding Author

John G. Labram − *School of Electrical Engineering and Computer Science, Oregon State University, Corvallis, Oregon 97331, United States;* orcid.org/0000-0001-6562-9895; Email: john.labram@oregonstate.edu

Author

Cinthya Trujillo Herrera − *School of Electrical Engineering and Computer Science, Oregon State University, Corvallis, Oregon 97331, United States*

Complete contact information is available at: https://pubs.acs.org/10.1021/acsaelm.1c00955

Author Contributions

J.G.L. conceived the project, devised strategy, carried out measurements, analyzed the data, developed theoretical models, implemented simulations, and wrote the paper. C.T.H. fabricated the devices. Both authors discussed the results and contributed to the writing of the paper.

Notes

The authors declare no competing financial interest.

■ ACKNOWLEDGMENTS

The authors thank the National Science Foundation for financial support (award number: 1942558). Part of this research was conducted at the Northwest Nanotechnology Infrastructure, a National Nanotechnology Coordinated Infrastructure site at Oregon State University, which is supported in part by the National Science Foundation (grant NNCI-2025489) and Oregon State University.

■ REFERENCES

(1) Posch, C.; Serrano-Gotarredona, T.; Linares-Barranco, B.; Delbruck, T. Retinomorphic Event-Based Vision Sensors: Bioinspired Cameras With Spiking Output. *Proc. IEEE* **2014**, *102* (10), 1470−1484.

(2) Guo, Y.; Liu, Y.; Oerlemans, A.; Lao, S.; Wu, S.; Lew, M. S. Deep Learning for Visual Understanding: A Review. *Neurocomputing* **2016**, *187*, 27−48.

(3) Yu, G.; Srdanov, G.; Wang, J.; Wang, H.; Cao, Y.; Heeger, A. J. Large Area, Full-Color, Digital Image Sensors Made with Semiconducting Polymers. *Synth. Met.* **2000**, *111*−*112*, 133−137.

(4) Adrian, E. D.; Matthews, R. The Action of Light on the Eye. *J. Physiol.* **1927**, *63* (4), 378−414.

(5) Hartline, H. K.; Graham, C. H. Nerve Impulses from Single Receptors in the Eye. *J. Cell. Comp. Physiol.* **1932**, *1* (2), 277−295.

(6) Trujillo Herrera, C.; Labram, J. G. A Perovskite Retinomorphic Sensor. *Appl. Phys. Lett.* **2020**, *117* (23), 233501.

(7) Snaith, H. J. Present Status and Future Prospects of Perovskite Photovoltaics. *Nat. Mater.* **2018**, *17* (5), 372−376.

(8) Snaith, H. J.; Abate, A.; Ball, J. M.; Eperon, G. E.; Leijtens, T.; Noel, N. K.; Stranks, S. D.; Wang, J. T.-W.; Wojciechowski, K.; Zhang, W. Anomalous Hysteresis in Perovskite Solar Cells. *J. Phys. Chem. Lett.* **2014**, *5* (9), 1511−1515.

(9) Frost, J. M.; Walsh, A. What Is Moving in Hybrid Halide Perovskite Solar Cells? *Acc. Chem. Res.* **2016**, *49* (3), 528−535.

(10) Lin, Y.-H.; Pattanasattayavong, P.; Anthopoulos, T. D. Metal-Halide Perovskite Transistors for Printed Electronics: Challenges and Opportunities. *Adv. Mater.* **2017**, *29* (46), 1702838.

(11) Labram, J. G.; Fabini, D. H.; Perry, E. E.; Lehner, A. J.; Wang, H.; Glaudell, A. M.; Wu, G.; Evans, H.; Buck, D.; Cotta, R.; Echegoyen, L.; Wudl, F.; Seshadri, R.; Chabinyc, M. L. Temperature-Dependent Polarization in Field-Effect Transport and Photovoltaic Measurements of Methylammonium Lead Iodide. *J. Phys. Chem. Lett.* **2015**, *6* (18), 3565−3571.

(12) Kim, H.; Gilmore, C. M.; Piqué, A.; Horwitz, J. S.; Mattoussi, H.; Murata, H.; Kafafi, Z. H.; Chrisey, D. B. Electrical, Optical, and Structural Properties of Indium−Tin−Oxide Thin Films for Organic Light-Emitting Devices. *J. Appl. Phys.* **1999**, *86* (11), 6451−6461.

(13) Cao, W.; Li, J.; Chen, H.; Xue, J. Transparent Electrodes for Organic Optoelectronic Devices: A Review. *J. Photonics Energy* **2014**, *4* (1), 040990−040991.

(14) Shirakawa, H.; Louis, E. J.; MacDiarmid, A. G.; Chiang, C. K.; Heeger, A. J. Synthesis of Electrically Conducting Organic Polymers: Halogen Derivatives of Polyacetylene, (CH) x. *J. Chem. Soc. Chem. Commun.* **1977**, No. 16, 578−580.

(15) Holliday, S.; Ashraf, R. S.; Wadsworth, A.; Baran, D.; Yousaf, S. A.; Nielsen, C. B.; Tan, C.-H.; Dimitrov, S. D.; Shang, Z.; Gasparini, N.; Alamoudi, M.; Laquai, F.; Brabec, C. J.; Salleo, A.; Durrant, J. R.; McCulloch, I. High-Efficiency and Air-Stable P3HT-Based Polymer Solar Cells with a New Non-Fullerene Acceptor. *Nat. Commun.* **2016**, *7* (1), 11585.

(16) Herrera, C. T.; Labram, J. G. Quantifying the Performance of Perovskite Retinomorphic Sensors. *J. Phys. Appl. Phys.* **2021**, *54* (47), 475110.

(17) Paterson, A. F.; Singh, S.; Fallon, K. J.; Hodsden, T.; Han, Y.; Schroeder, B. C.; Bronstein, H.; Heeney, M.; McCulloch, I.; Anthopoulos, T. D. Recent Progress in High-Mobility Organic Transistors: A Reality Check. *Adv. Mater.* **2018**, *30* (36), 1801079.

(18) Herz, L. M. Charge-Carrier Mobilities in Metal Halide Perovskites: Fundamental Mechanisms and Limits. *ACS Energy Lett.* **2017**, *2* (7), 1539−1548.

(19) Sze, S. M.; Ng, K. K. *Physics of Semiconductor Devices*; John Wiley & Sons, 2006.

(20) Vezie, M. S.; Few, S.; Meager, I.; Pieridou, G.; Dörling, B.; Ashraf, R. S.; Goñi, A. R.; Bronstein, H.; McCulloch, I.; Hayes, S. C.; Campoy-Quiles, M.; Nelson, J. Exploring the Origin of High Optical Absorption in Conjugated Polymers. *Nat. Mater.* **2016**, *15*, 746−753.

(21) Nelson, J. Polymer:Fullerene Bulk Heterojunction Solar Cells. *Mater. Today* **2011**, *14* (10), 462−470.

(22) Gao, F.; Koster, L. J. A.; Nguyen, T.-Q.; Stingelin, N. Organic Photovoltaics. *Adv. Energy Mater.* **2018**, *8* (28), 1802706.

(23) Trujillo Herrera, C.; Hong, M. J.; Labram, J. G. Role of the Blend Ratio in Polymer:Fullerene Phototransistors. *ACS Appl. Electron. Mater.* **2020**, *2* (7), 2257−2264.

(24) Noriega, R.; Rivnay, J.; Vandewal, K.; Koch, F. P. V.; Stingelin, N.; Smith, P.; Toney, M. F.; Salleo, A. A General Relationship between Disorder, Aggregation and Charge Transport in Conjugated Polymers. *Nat. Mater.* **2013**, *12* (11), 1038−1044.
(25) Kovacik, P.; Assender, H. E.; Watt, A. A. R. Morphology Control in Co-Evaporated Bulk Heterojunction Solar Cells. *Sol. Energy Mater. Sol. Cells* **2013**, *117*, 22−28.
(26) Arias, A. C.; MacKenzie, J. D.; McCulloch, I.; Rivnay, J.; Salleo, A. Materials and Applications for Large Area Electronics: Solution-Based Approaches. *Chem. Rev.* **2010**, *110* (1), 3−24.
(27) Nielsen, C. B.; Holliday, S.; Chen, H.-Y.; Cryer, S. J.; McCulloch, I. Non-Fullerene Electron Acceptors for Use in Organic Solar Cells. *Acc. Chem. Res.* **2015**, *48* (11), 2803−2812.
(28) Dang, M. T.; Hirsch, L.; Wantz, G. P3HT:PCBM, Best Seller in Polymer Photovoltaic Research. *Adv. Mater.* **2011**, *23* (31), 3597−3602.
(29) Shuttle, C. G.; O'Regan, B.; Ballantyne, A. M.; Nelson, J.; Bradley, D. D. C.; Durrant, J. R. Bimolecular Recombination Losses in Polythiophene: Fullerene Solar Cells. *Phys. Rev. B* **2008**, *78* (11), 113201.
(30) Lakhwani, G.; Rao, A.; Friend, R. H. Bimolecular Recombination in Organic Photovoltaics. *Annu. Rev. Phys. Chem.* **2014**, *65* (1), 557−581.
(31) Juška, G.; Genevičius, K.; Nekrašas, N.; Sliaužys, G.; Dennler, G. Trimolecular Recombination in Polythiophene: Fullerene Bulk Heterojunction Solar Cells. *Appl. Phys. Lett.* **2008**, *93* (14), 143303.
(32) Liu, C.; Xu, Y.; Noh, Y.-Y. Contact Engineering in Organic Field-Effect Transistors. *Mater. Today* **2015**, *18* (2), 79−96.
(33) Levine, I.; Gupta, S.; Brenner, T. M.; Azulay, D.; Millo, O.; Hodes, G.; Cahen, D.; Balberg, I. Mobility−Lifetime Products in MAPbI3 Films. *J. Phys. Chem. Lett.* **2016**, *7* (24), 5219−5226.
(34) Labram, J. G.; Perry, E. E.; Venkatesan, N. R.; Chabinyc, M. L. Steady-State Microwave Conductivity Reveals Mobility-Lifetime Product in Methylammonium Lead Iodide. *Appl. Phys. Lett.* **2018**, *113* (15), 153902.
(35) Balberg, I. The Two Carriers' Mobility-lifetime Products and Their Light Intensity Dependencies in Hydrogenated Amorphous Silicon. *J. Appl. Phys.* **1994**, *75* (2), 914−923.
(36) Chua, L.-L.; Zaumseil, J.; Chang, J.-F.; Ou, E. C.-W.; Ho, P. K.-H.; Sirringhaus, H.; Friend, R. H. General Observation of N-Type Field-Effect Behaviour in Organic Semiconductors. *Nature* **2005**, *434* (7030), 194−199.
(37) Anthopoulos, T. D.; Singh, B.; Marjanovic, N.; Sariciftci, N. S.; Montaigne Ramil, A.; Sitter, H.; Cölle, M.; de Leeuw, D. M. High Performance N-Channel Organic Field-Effect Transistors and Ring Oscillators Based on C60 Fullerene Films. *Appl. Phys. Lett.* **2006**, *89* (21), 213504.
(38) Ostroverkhova, O. Organic Optoelectronic Materials: Mechanisms and Applications. *Chem. Rev.* **2016**, *116* (22), 13279−13412.
(39) Miranda, P. B.; Moses, D.; Heeger, A. J. Ultrafast Photogeneration of Charged Polarons in Conjugated Polymers. *Phys. Rev. B* **2001**, *64* (8), 081201.
(40) Hwang, I.-W.; Moses, D.; Heeger, A. J. Photoinduced Carrier Generation in P3HT/PCBM Bulk Heterojunction Materials. *J. Phys. Chem. C* **2008**, *112* (11), 4350−4354.
(41) Pivrikas, A.; Neugebauer, H.; Sariciftci, N. S. Charge Carrier Lifetime and Recombination in Bulk Heterojunction Solar Cells. *IEEE J. Sel. Top. Quantum Electron.* **2010**, *16* (6), 1746−1758.

https://doi.org/10.1021/acsaelm.1c00955
ACS Appl. Electron. Mater. XXXX, XXX, XXX−XXX